

GT2016-57652

STEAM TURBINE ROTOR TRANSIENT THERMO-STRUCTURAL ANALYSIS AND LIFETIME PREDICTION

Dr. Leonid Moroz

SoftInWay Inc.

15 New England Executive Park
Burlington, MA 01803, USA

L.Moroz@softinway.com

Dr. Boris Frolov

SoftInWay Inc.

15 New England Executive Park
Burlington, MA 01803, USA

boris.frolov@softinway.com

Dr. Roman Kochurov

SoftInWay Inc.

15 New England Executive Park
Burlington, MA 01803, USA

R.Kochurov@softinway.com

ABSTRACT

Market requirements for faster and more frequent power unit start-up events result in a much faster deterioration of equipment, and a shorter equipment lifespan. Significant heat exchange occurs between steam and turbine rotors during the start-up process and even more intensive heat exchange takes place during the condensation phase in cold start-up mode, which leads to further thermal stresses and lifetime reduction. Therefore, the accuracy of lifetime prediction is strongly affected and dependent on the accuracy of transient thermal state prediction.

In this study, transient thermal and structural analyses of a 30 MW steam turbine for a combined High and Intermediate pressures (HPIP) rotor during a full cold start cycle is performed and special attention is paid to initial start-up phase with 'condensation' thermal BC. All steps for rotor design and the thermal model preparation were done using the AxSTREAM™* software platform. It included the development of a two dimensional model of the rotor, thermal zones and corresponding thermal boundary conditions (heat transfer coefficients and steam temperatures) calculation during turbine start-up and shut down operation. Rotor thermal and structural simulations were done using commercial FE analysis software to evaluate the thermo-stress-strain state of the turbine rotor. Calculation and validation of thermal and structural state of the rotor was done using actual start-up cycle and measured data from a power plant, and it showed good agreement of the calculated and

the measured data. Based on the results of thermo-structural analysis, the evaluation of rotor lifetime by means of a low cycle fatigue approach was performed and presented in this paper.

NOMENCLATURE

BC – boundary conditions

FE – finite element

FEA – finite element analysis

HP – high pressure

HTC – heat transfer coefficient

IP – intermediate pressure

LCF – low cycle fatigue

Re – Reynold's number

Pr – Prandtl number

INTRODUCTION

During load transients, biaxial thermal strains are created as a result of the radial temperature gradient through the thickness of the rotor. During start-ups, the outer surface heats up faster than the bore or centerline. Compressive stresses appear in the outer surface of the shaft while tensile stresses are created at the bore/centerline. During shut downs, the opposite takes place; the outer surface is subject to tensile thermal stress (as it cools more rapidly than the bulk of the rotor mass) and the bore/centerline is subject to compressive thermal stress. Generally speaking, thermal stress/strain is proportional to the rate of temperature change and the square of the shaft diameter.

Turbine operators want quick starts to maximize output. Operators also expect long service life. These two requirements

* AxSTREAM™ is trademark product of SoftInWay Inc.

are conflicting because starting the turbine too quickly can result in premature component failure due to LCF cracking. Prior to the mid-1960s, the relationship between quick starts and LCF was not well understood in the industry. LCF cracking of high temperature rotors primarily at the shaft/wheel fillet as a result of rapid, uncontrolled starts and stops was common. During the mid-1960s, major OEMs began to provide customers with thermal loading (i.e ramp rate) guidelines and general starting and loading recommendations in the form of basic station starting and loading procedures. Later, electronic controllers for large fossil fired steam turbines included load change logic that would “select” a ramp rate based on an internal LCF calculation algorithm.

Today’s steam turbine rotor designer must be well informed about the overall controlling method, boiler characteristics, and any special pre-determined start up time or cycle requirements imposed by the customer or product specifications. From these, a “mission mix” representing the expected cyclic life of the steam turbine can be generated and evaluated based on the deterministic methods.

Turbine cyclic life could be limited by either component – rotor or stator- but in this article, considering limited size of the publication, we will present the results for a turbine rotor only.

Cyclic life evaluation is based on thermo-stresses analysis and requires a high level of FE model detailing in order to capture stresses concentration in the rotor elements, like fillets, grooves, etc.

For differential expansion and clearances design, thermal expansion analysis for both components (casing and rotor) is required. In this study the level of FE model detailing does not need to be as high as at a stresses study.

Steam turbine transient operation is usually very complex with regards to thermo-mechanical state prediction, which usually consists of the following major steps for start-up:

- flow path parameters and heat exchange conditions calculation (HTC’s and steam temperatures);
- thermal analysis;
- thermo-structural analysis;
- lifetime evaluation.

Intensity of heat exchange and consequently thermal stresses significantly increase in case of phase change effect, when rotor surface temperature is lower than steam saturation temperature. The condensation process typically takes place at the initial phase of the start-up cycle and continues until the rotor surface temperature becomes higher than that of the steam saturation temperature. This situation is characterized by condensation heat exchange conditions with increased level of HTC’s on the rotor surface. Fundamentals of heat and mass transfer processes and basic principles of HTC simulation are considered in the monographs [1, 2]. Unfortunately, there are not many recommendations available on condensation HTC methodology for steam turbines and this effect imposes most of the uncertainty that exists for rotor thermo-structural analysis. A theoretical approach to account for the effect of condensation on HTC and validation against test data is presented and discussed in [3]. Some recommendations based on a summary of calculated

and experimental data are presented in [4], and based on these results the condensation HTC are significantly higher than that of dry conditions and could reach up to 12000 [W/(m²K)].

High HTC’s during the condensation phase of the start-up lead to high thermal gradients, resulting in thermal stresses (thermal shock) and finally resulting in rotor lifetime reduction and early damage.

Numerous studies for thermo-mechanical analyses methodology with FEA approach have been developed and published recently in [5-12]. These and many other publications represent different aspects of thermo-structural analysis and turbine components behavior – FE model development, zones for heat transfer condition definition and HTC assignment, critical regions in turbine components, thermo-stresses during turbine transient operation, plasticity effect, life-time estimation methods, etc. At the same time, in the openly published works, not enough attention is paid to the effect of condensation and its impact on thermo-structural stresses and cyclic life. This is one of the methodological aspects which we would like to focus on and discuss in this article.

1. ROTOR DESIGN AND THERMO-STRUCTURAL ANALYSIS METHODOLOGY

During a 30 MW steam turbine upgrade project, the full scope of mechanical analyses was performed for an HPIP rotor including a thermo-structural study on transient regimes and lifetime estimation. The HPIP cylinder cross section view is shown in Fig. 1.

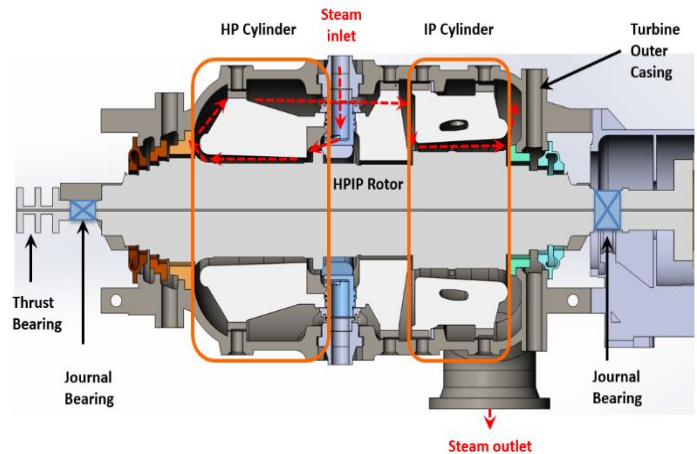


Figure 1: 30MW Steam Turbine HPIP Components

In general, thermo-structural analysis is a vital part of the rotor design process, which involves numerous algorithms and sub steps, with interaction between them (see Fig. 2).

The full scope of rotor design activities are presented in the flowchart in Fig. 2, where rotor geometry generation is done with some design modules, marked with blue rectangle, and modules involved in rotor thermo-structural analyses, marked with the red rectangle.

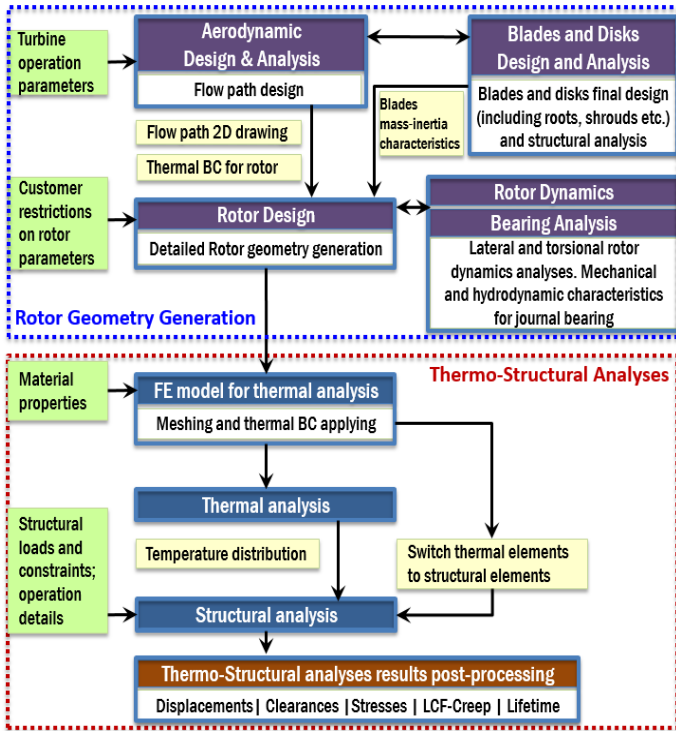


Figure 2: Rotor Design and Analysis Process Flow Chart

After full rotor geometry is determined, thermal BC at main flow path, shaft packing zones and rotor ends/bearings zones are calculated and automatically transferred to the rotor thermo-structural FE model. The next step is thermo-structural analysis to determine displacements and stresses, and finally lifetime estimation based on thermal and structural results.

All design steps involved in rotor geometry preparation and BC generation are done within the integrated design and analysis modules and corresponding thermo-structural analyses steps are performed in commercial FEA software with automatic data exchange between these two parts. The advantage of such an integrated iterative approach is the automation of the design process where thermal BC determination and application to FE model at each time step of start-up cycle is done by leveraging the automatically generated macro. Such an approach significantly improves the accuracy of thermo-structural prediction by means of local thermal zones/time steps refinement and accelerates the whole design/analysis process.

Heat transfer modelling and thermal analysis.

To simulate heat convection conditions, the rotor surface is split into thermal zones with convection conditions identical within each zone. Thermal BC's were determined taking into account local physics of the flow. Figure 3 shows thermal BC zone assignments for a typical reaction steam turbine stage.

Heat transfer for rotor surfaces is based on the classical approach [1 – 3] and given by the Dittus-Boelter equation for turbulent pipe flow as follows:

$$Nu = 0.023 \cdot Re^{0.8} \cdot Pr^{0.333}$$

$$HTC = Nu \cdot k/D_h, \quad (1)$$

where $Re = V_{tot} \cdot D_h / (\mu \cdot V)$;

V_{tot} – velocity of steam relative to rotor surface;

$$V_{tot} = \sqrt{V_{ax}^2 + V_{rel}^2}; V_{rel}^2 = XK \cdot \omega \cdot r; V_{ax}^2 = \frac{G}{\pi \rho (r_{ext}^2 - r_{in}^2)};$$

XK – coefficient, which considers influence of velocity profile in the gap between rotating and non-rotating surfaces;

ω – rotational speed;

r – cylindrical surface radius;

G – steam mass flow rate;

ρ – steam density;

r_{ext} – external surface radius;

r_{in} – internal surface radius;

D_h – hydraulic diameter;

μ – steam viscosity;

V – specific volume;

k – thermal conductivity.

Local flow properties are determined from aerodynamic code.

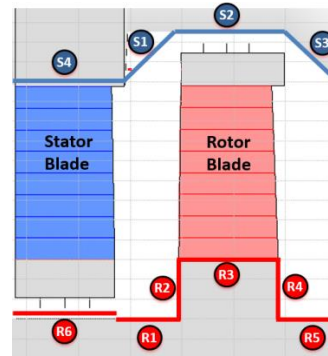


Figure 3: Flow Path Stage Heat Convection Zones Schematization

Rotor end seals and corresponding thermal zones are presented in Fig. 4. Thermal BC was assigned to journal and thrust bearings surfaces.

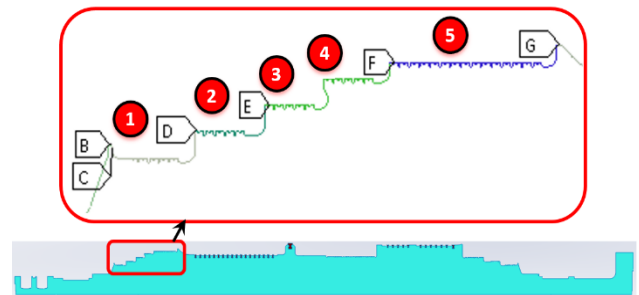


Figure 4: Rotor End Seals Heat Convection Zones Schematization

To account for the effect of condensation, two types of thermal conditions are considered – ‘non-condensing’ and ‘condensing’. ‘Non-condensing’ conditions are determined by the above mentioned equation (1). For ‘condensing’ BC, a different approach for HTC is used [3, 4] and, for temperature – steam saturation, temperature is considered.

The initial rotor temperature field is determined by previous turbine operation status – cold, warm or hot and used to start calculation process. To account for the effect of condensation, the algorithm in Fig. 5 is proposed. If saturation temperature for any zone is higher than that of rotor metal temperature, we assume that a condensation process occurs. In this case, HTC for condensation and steam saturation temperature is applied to this zone. Such an approach allows the monitoring of the rotor thermal state during the heating process and allows us to distinguish the condensation phenomenon with a high level of accuracy with setting ‘condensing’ vs. ‘non-condensing’ thermal boundary conditions for each local zone at each moment in time.

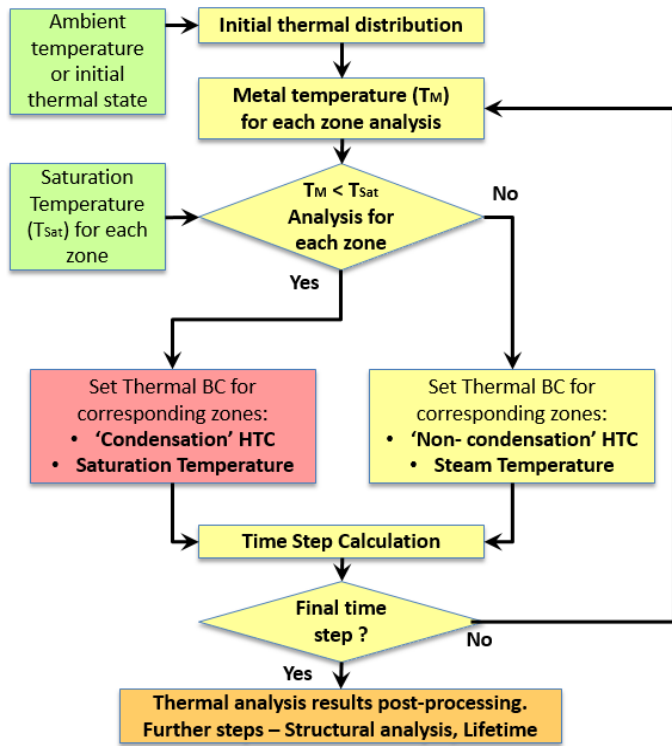


Figure 5: Interactive Algorithm for Thermal ‘Condensing’ / ‘Non-condensing’ BC Set Up for Transient Analysis

Structural Analysis.

Structural analysis was done in linear (elastic) and non-linear (plasticity effect) formulations based on the calculated rotor thermal state during a cold start process.

Elastic stress analysis was performed as a preliminary step to determine the level of stresses and critical time periods for more detailed plastic analysis. Plastic analysis is critical to time steps and requires much more computation resources. Such an approach helps to optimize the algorithm of nonlinear plastic

analysis and therefore improve accuracy and reduce overall calculation time.

For plastic analysis, a multi-linear kinematic hardening plasticity model is used. The rotor material is cyclically hardened. The non-linear analysis model includes the Baushinger effect and geometrical nonlinearity to get physically accurate results.

LCF analysis methodology is based on rotor thermo-mechanical stress-strain state prediction in non-linear plastic statement and experimental strain-life (ϵ -N) curves for rotor material during a cold start-up cycle.

2. STEAM TURBINE HPIP ROTOR FINITE ELEMENT MODEL

HPIP turbine rotor nominal speed is 3600 rpm. Steam inlet temperature is 520 °C. The rotor is manufactured from 20H3MV steel. Main characteristics of the rotor material are presented in the table 1 below.

Table 1. Main material properties for rotor steel

Temp.	Density	Young modulus	Coeff. of linear expansion (20 - T)	Thermal conduction coeff.	Specific heat (20 - T)	Poisson's ratio
T, °C	ρ , kg/m ³	E, 10 ⁻⁵ MPa	α , 10 ⁶ 1/C	λ , W/(m·°C)	C, J/(kg·°C)	ν
20	7800	2.11		38.5		0.3
100		2.04	10.6	35.6	502	
400		1.90	12.1	30.6	650	
500		1.81	12.6	29.7	710	

To include plasticity effect in the rotor model, the family of stress-strain curves at room and elevated temperatures are used as an input for structural analysis. Stress-strain curves for 20H3MV steel at room and elevated temperatures are shown in Fig. 6 below.

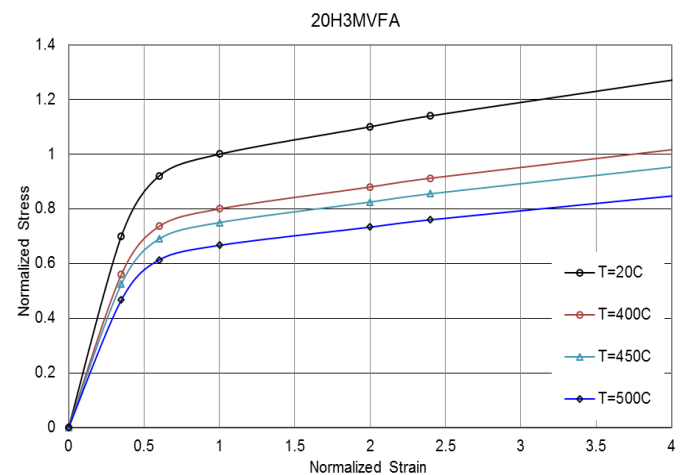


Figure 6: 20H3MVFA steel stress-strain curves

A rotor axisymmetric 2D model with 8-node quadrilateral plane elements (with axisymmetric option) is used for transient thermal and structural FE analyses. Mesh refinement was done in the regions of potential stress concentration – disk fillets, dovetail grooves, etc. FEA mesh for HPIP rotor is shown in Fig. 7.

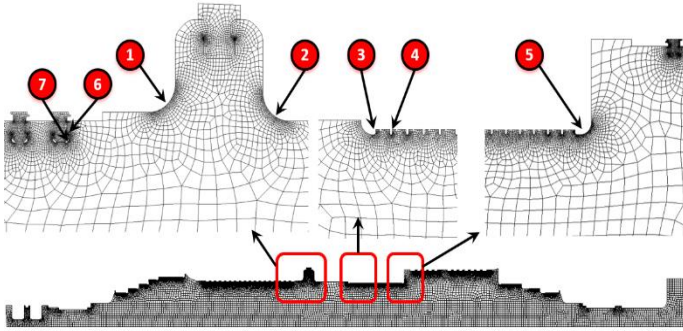


Figure 7: FE Mesh for 30MW Steam Turbine HPIP Rotor

Rotor regions with anticipated maximal thermal gradients and stresses (critical zones with regards to LCF crack initiation) are indicated by numbers 1 – 7 in Fig. 7 for further detailed analyses.

3. ROTOR TRANSIENT THERMO-STRUCTURAL ANALYSIS RESULTS AND DISCUSSION

Thermal Analysis.

For transient thermal analysis, cold start-up and shut down operations are considered. A cold start-up diagram for the turbine is presented in Fig. 8 below.

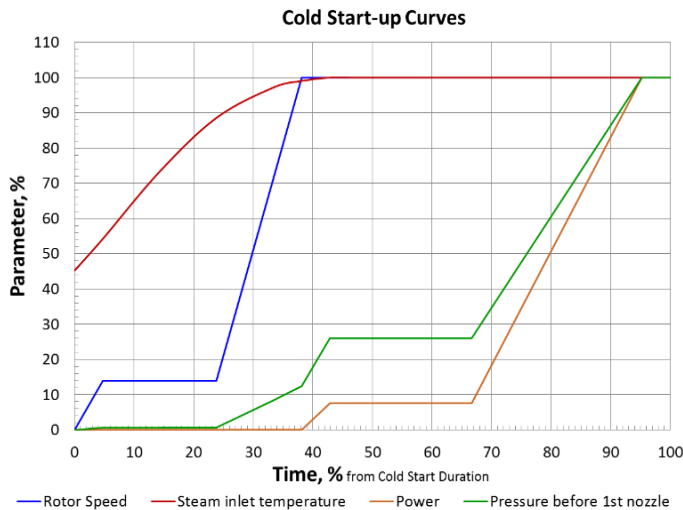


Figure 8: Cold Start-up Diagram

Calculated rotor temperature distributions during cold start up and steady state operation are presented in Fig. 9.

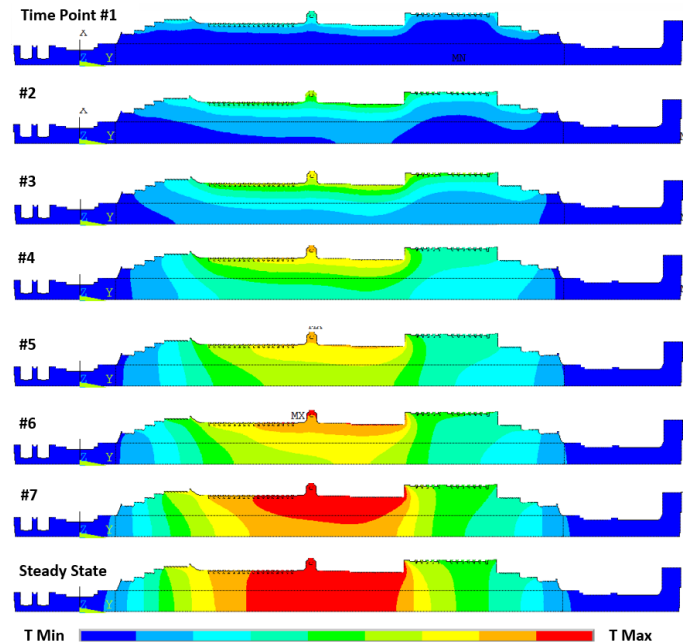


Figure 9: Rotor Temperatures During a Cold Start up and Steady State Operation

The rise of the rotor metal temperature takes place at all times, starting from initial moment up to steady state operation. The rotor thermal distribution varies in both radial and axial directions during start-up, while during steady state operation the thermal distribution is almost axial.

Structural Analysis.

Structural boundary conditions, centrifugal rotor/blading and pressure loads are considered in the analysis. Transient temperature distribution, calculated earlier, is applied to the structural rotor FE model as the thermal load at appropriate time steps.

Elastic structural analysis provides accurate results for the linear thermal expansion problem. Figure 10 represents rotor thermal expansion during steady state operation.

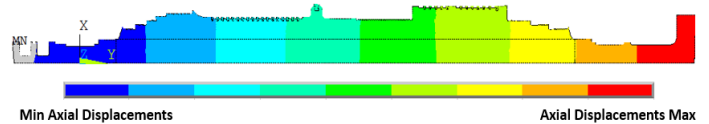


Figure 10: Rotor Linear Thermal Expansion at Full Load Steady State Operation

Validation of the thermo-structural algorithm was done through a comparison with measured data during the turbine commissioning phase. As thermocouples were installed only on the turbine casing components, the rotor temperature field was not measured and validation was done against rotor expansion.

Comparison for rotor thermal expansion (maximum displacement) is presented in Fig. 11, which shows good agreement between calculated and measured data (less than 5% error).

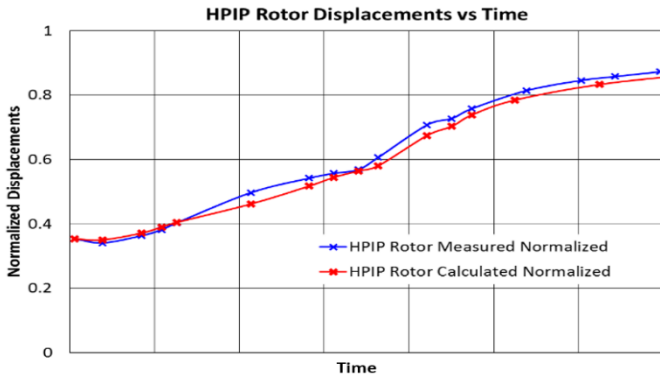


Figure 11: Rotor Linear Thermal Axial Expansion during Cold Start-up

The thermal gradients cause thermal stresses which can be observed during transient and steady state operation and contribute a significant portion of stresses in entire stress-strain state. Two cycles of rotor transient plastic stress analyses were performed for start-up – running – shut down operations to reach stabilized stress-strain hysteresis loops for each region of interest.

Both variants of stress analyses – linear and non-linear – have been performed and compared. As an example, calculated linear and non-linear stresses versus time at cold start-up for point #2 (see Fig. 7) are presented in Fig. 12. This plot also demonstrates logic to select calculation time steps duration for non-linear analysis. Time steps duration is determined based on elastic stress gradients – short time steps correspond to high stress gradients and longtime steps is for low stress gradients.

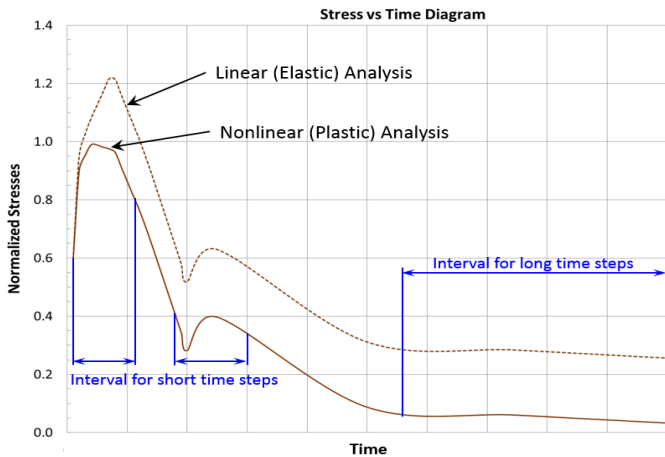


Figure 12: Equivalent Stresses During Cold Start-up at Critical Point #2 Calculated using Linear and Non-linear Analysis

Equivalent stress (plastic study) versus time for critical regions #1 – #5 (see Fig. 7 for details) are represented in Fig. 13 by solid lines, and temperatures are represented by dashed lines with corresponding colors. Points on the time axis in Fig. 13 correspond to time points in Fig. 9.

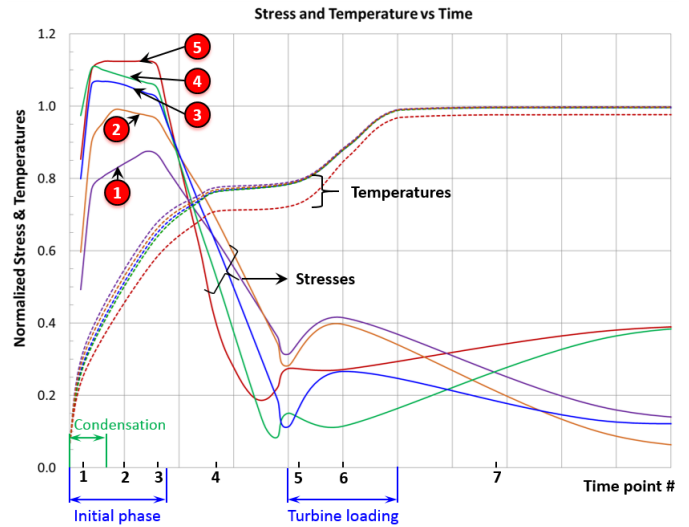


Figure 13: Equivalent Stresses During Cold Start-up at Critical Points

Equivalent stress (plastic study) distribution during cold start-up and steady state operation is presented in Fig. 14.

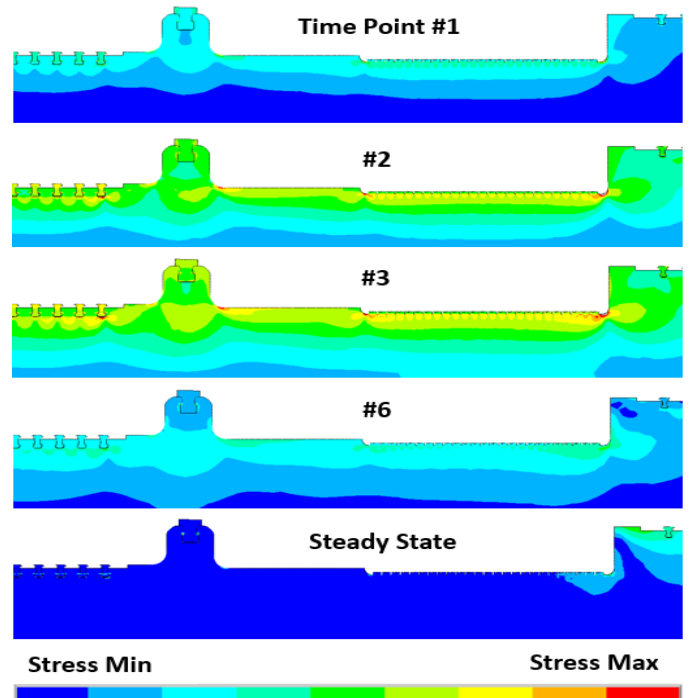


Figure 14: Equivalent Stresses Distribution During Cold Start-up

Thermal gradients contribute the main portion of stresses into the entire stress-strain state of the HPIP turbine rotor. The highest level of thermal gradients and stresses can be observed in the early phase of the cold start-up process, when steam condensation takes place, marked by green line in Fig. 13. Analysis shows that the thermal shock at this period is more critical than at all following start-up steps. Another critical moment is the turbine loading phase, which also contributes to stress increases, although stresses are lower than at the condensation phase. The peak stresses appear on the disk fillets in the region of steam inlet (points 1 and 2 from Fig. 7), on HP-IP middle seal (points 3, 4, 5), and 1st stage HP blade grooves (corresponding points 3, 4, 6, 7). Maximal stresses correspond to point 5. The calculated level of stresses for the HPIP steam turbine rotor in all mentioned regions of stress concentrators is above the yield limit.

Low Cycle Fatigue Analysis.

The varying stresses in the HPIP rotor lead to deterioration processes in the component material, resulting in thermo-mechanical fatigue. In addition to the mentioned fatigue mechanism, in the high temperature applications, creep is another contributor to limited rotor lifetime. The current study is focused on LCF mechanism only to determine the number of cycles to failure.

Low cycle fatigue analysis is based on fatigue test data at elevated temperatures for the rotor material and thermo-structural non-linear analysis results, presented above. The experimental strain – life (ϵ -N) curve for 20H3MVFA steel is presented in Fig. 15.

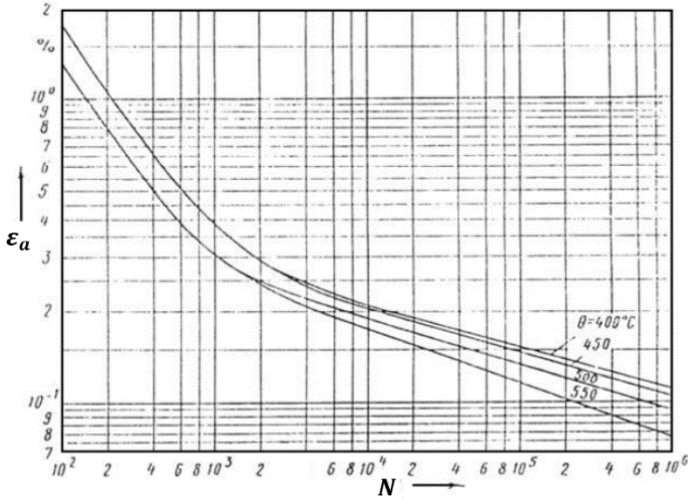


Figure 15: Strain – Life Curve for 20H3MVFA steel

To determine the expected rotor life, an effective strain range ($\Delta\epsilon_{eff}^{tot}$) [13] is calculated for rotor critical zones (corresponding nodes from FE model) according to the equations (2) below:

$$\Delta\epsilon_{eff}^{el} = \frac{\sqrt{2}}{2(1+\nu)} \left[\begin{aligned} &(\Delta\epsilon_{xx}^{el} - \Delta\epsilon_{yy}^{el})^2 + (\Delta\epsilon_{yy}^{el} - \Delta\epsilon_{zz}^{el})^2 + \\ &+ (\Delta\epsilon_{zz}^{el} - \Delta\epsilon_{xx}^{el})^2 + \\ &+ \frac{3}{2}(\Delta\gamma_{xy}^{el2} + \Delta\gamma_{yz}^{el2} + \Delta\gamma_{zx}^{el2}) \end{aligned} \right]^{1/2};$$

$$\Delta\epsilon_{eff}^{pl} = \frac{\sqrt{2}}{3} \left[\begin{aligned} &(\Delta\epsilon_{xx}^{pl} - \Delta\epsilon_{yy}^{pl})^2 + (\Delta\epsilon_{yy}^{pl} - \Delta\epsilon_{zz}^{pl})^2 + \\ &+ (\Delta\epsilon_{zz}^{pl} - \Delta\epsilon_{xx}^{pl})^2 + \\ &+ \frac{3}{2}(\Delta\gamma_{xy}^{pl2} + \Delta\gamma_{yz}^{pl2} + \Delta\gamma_{zx}^{pl2}) \end{aligned} \right]^{1/2}; \quad (2)$$

$$\Delta\epsilon_{eff}^{tot} = \Delta\epsilon_{eff}^{el} + \Delta\epsilon_{eff}^{pl},$$

where ϵ_{ij}^{el} , ϵ_{ij}^{pl} , γ_{ij}^{el} , γ_{ij}^{pl} – elastic and plastic strain components; and $\Delta\epsilon_{ij}^{el/pl} = \epsilon_{ij\ MAX}^{el/pl} - \epsilon_{ij\ MIN}^{el/pl}$, calculated on loading cycle.

Additional correction for stresses in the asymmetrical cycle was applied using following formula (3):

$$\Delta\epsilon'_{eff\ tot} = \frac{\Delta\epsilon_{eff\ tot}}{1 - \frac{\sigma_{avr}}{\sigma_{ult}}}, \quad (3)$$

where σ_{avr} – average stresses in a cycle, σ_{ult} – ultimate strength.

Taking into account safety factors that are affected by inaccuracy of calculation methodology, level of uncertainty in material properties, possible deviation in steam parameters, etc., the number of cycles to failure N can be calculated according to the following approach:

$$N_{aN} = \frac{N(\epsilon_a)}{K_N}; \quad N_{a\epsilon} = N(\epsilon_a K_\epsilon);$$

$$N = \min\{N_{aN}, N_{a\epsilon}\}, \quad (4)$$

where ϵ_a – strain amplitude, K_N , K_ϵ – safety factors, $N(\epsilon_a)$, $N(\epsilon_a K_\epsilon)$ – number of cycles to failure calculated using strain – life (ϵ -N) curve.

Effective strain range calculations show that the most critical region is the local zone #5 (Fig. 7), where $\Delta\epsilon'_{eff\ tot}$ is 0.54%. With this parameter, determined from thermo-structural analysis and considering effect of safety factors – see equation (4), the number of cold starts is limited to 1000 cycles.

CONCLUSIONS

The proposed method allows us to account for ‘condensation’ vs. ‘non-condensation’ steam thermal conditions. A high level of automation during all analysis steps helps to accelerate the whole process and improve calculation accuracy. The validation of the proposed method has been done for rotor thermal expansion against field test data which shows good agreement and prove acceptable accuracy of proposed methodology for engineering tasks.

Leveraging this life cycle prediction methodology 30MW steam turbine HPIP rotor upgrade has been performed and a number of cold start-up cycles have been estimated.

The next step of this work, which is currently in progress, is dedicated to a casing thermo-structural analysis and rotor-to-

casing differential expansion study. This portion of work is planned to be presented in a future publication.

REFERENCES

- [1] Incropera, F.P., Dewitt, D.P., 1996, 'Fundamentals of Heat and Mass Transfer', 5th Ed., John Wiley & Sons, Inc., New York, N.Y.
- [2] Kreith F., 1973, 'Principles of Heat Transfer', 3rd Ed., IEP-A Dun-Donnelley, New York, N.Y.
- [3] Matsevity Yu. M., Alyokhina S. V., Goloschapov V. N., Kotulskaja O. V., 2012, 'Heat exchange in construction of steam turbines elements', NAS of Ukraine, A. N. Podgorny Institute for Mechanical Engineering Problems. – Kharkiv. – in rus.
- [4] Uche J., Artal J., Serra L., 2002, 'Comparison of heat transfer coefficient correlations for thermal desalination units', *Desalination*, Vol. 152.
- [5] Brilliant, H. M., Tolpadi, A. K., 2004, 'Analytical approach to steam turbine heat transfer in a combined cycle power plant', *ASME Turbo Expo*, Vienna, Austria. GT2004-53387.
- [6] Marinescu G, Ehram A, Sell M, Brunner P., 2013, 'Experimental Investigation in Thermal Behavior of Steam Turbine Components: Part 3—Startup and the impact of LCF life', *ASME Turbo Expo*, San Antonio, Texas, USA. GT2013-94356.
- [7] Topel M, Jöcker M, Paul S, Laumert B., 2015, 'Differential expansion sensitivity studies during steam turbine start-up', *ASME Turbo Expo*. Montréal, Canada. GT2015-42214.
- [8] Wang W.Z., Zhang J.H., Liu H.F., Liu Y.Z., 2014, 'Influence of creep on low-cycle fatigue life assessment of ultrasupercritical steam turbine rotor', *ASME Turbo Expo*, Düsseldorf, Germany. GT2014-26757.
- [9] Mao J., Wang W., Liu Y., Zhang J., 2012, 'Multiaxial creep-fatigue life prediction on the rotor of a 1000MW supercritical steam turbine', *ASME Turbo Expo*, Copenhagen, Denmark. GT2012-69135.
- [10] Chen R., He A P., Yang Y. L., Ye X. Z., Jiang P. N., Hua W. X., 2013, 'Life Assessment Technology of Steam Turbine Rotor', *ASME Turbo Expo*, San Antonio, Texas, USA. GT2013-95456.
- [11] Mukhopadhyay D., Brilliant, H. M., Zheng X., 2014, 'Development of a conjugate heat transfer simulation methodology for prediction of steam turbine cooldown phenomena and shell deflection', *ASME Turbo Expo*, Düsseldorf, Germany. GT2014-25874.
- [12] Hu Y., Jiang P., Ye X., Chen G., Zhang J., Hao Z., Xiao L., 2015, 'Lifetime Assessment of Steam Turbine Casing', *ASME Turbo Expo*, Montréal, Canada. GT2015-43495.
- [13] ASME Boiler & Pressure Vessel Code, 2008, American Society of Mechanical Engineers. New York, N.Y.